Lattice Boltzmann Modeling for Natural Convection in a Square Cavity Partially Heated and Filled with a Non-Newtonian Fluid: Analysis of Combined Effects of a Magnetic Field and Internal Heat Generation

Khalid Chtaibi[1,2(✉)], Mohammed Hasnaoui[1], Haïkel Ben Hamed[2], Youssef Dahani[1], and Abdelkhalek Amahmid[1]

[1] Laboratory of Fluid Mechanics and Energetics (LMFE), Unit Affiliated to CNRST, Department of Physics, Faculty of Sciences Semlalia, UCA, BP 2390, Marrakesh, Morocco
khalid.chtaibi@edu.uca.ac.ma

[2] UPJV, University Institute of Technology, LTI, Amiens, France

Abstract. The combined impact of a Lorentz force and volumetric heat generation on natural convection heat transfer and fluid flow in a square cavity are investigated numerically using MRT-LBM. The cavity is filled with a non-Newtonian fluid and submitted to a partial heating from below. The main physical parameters controlling the problem are the Hartmann number ($0 \leq Ha \leq 50$), the external Rayleigh number ($Ra_E = 10^5$), the parameter characterizing the intensity of heat generation ($R = 0$ and 1), and the power-law index ($0.8 \leq n \leq 1.2$). The findings of the present study are illustrated by presenting streamlines, isotherms, and mean Nusselt numbers.

Keywords: Lattice Boltzmann method · Non-Newtonian fluid · Natural convection · Magnetic field · Volumetric heat generation

1 Introduction

Heat transfer by natural MHD convection in cavities heated from below and confining non-Newtonian fluids is an important area of research due to its involvement in many practical and industrial domains, including the medical and chemical industries, as well as the polymer and food processing [1]. The damping role of the magnetic field allows to modulate the thermally generated melting front [2] and its effect is controlled by the strength of the applied magnetic field through the Hartmann number. Many past studies have been conducted to investigate natural convection heat transfer of non-Newtonian fluids under the effect of an external magnetic field. The impact of the strength of the latter and the tilt angle of the confining configurations on heat transfer by natural convection in linearly heated [3], partially heated [4], and differentially heated [5] square cavities has been examined. The results presented in these studies show a considerable impact of the

F. Ali-Toudert et al. (Eds.): JITH 2022, LNME, pp. 100–110, 2024.
https://doi.org/10.1007/978-3-031-43934-6_11

power-law index and the Hartmann number on heat transfer. More recently, Aghakhani et al. [6] employed the FD-LBM (Lattice Boltzmann-Finite Difference) approach to investigate the heat transfer of a non-Newtonian fluid by natural convection in a C-shaped enclosure submitted to the action of a horizontal magnetic field. Their findings reveal that the influence of convection becomes more important as the Rayleigh number increases, and that it is much more relevant for a shear-thinning fluid. However, raising the Hartmann number has a detrimental influence on fluid flow and heat transfer for various rheological behaviors. Similar findings have been reported by Zhang et al. [7] in an L-shaped cavity.

The literature review shows that natural convection in enclosures heated by internal heat sources has been the object of many studies [8–10]. This interest stems in part from the wide variety of important applications in different fields covering among others solar energy harvesting and operation, nuclear reactor safety, and fire prevention. The presence of internal heat generation provides additional dynamics in convective flow systems and may lead to unexpected behaviors. Thus, the effect of heat generation/absorption in the presence/absence of an external magnetic field on heat transfer generated by natural convection has been reported in some prior studies. In this frame, Khanafer et al. [11] studied numerically the magnetic field influence on the heat transfer generated by free convection in an inclined square cavity saturated with a porous media. Their results confirm the attenuation of the natural convection effect that results from the increase of Hartmann number. Recently, the Lattice Boltzmann method has been used to study the heat generation influence on heat and mass transfer and fluid flow by Soret driven free convection in the absence of the Lorentz force both in steady [12] and unsteady [13] flow regimes. The results of these studies show that heat generation impacts significantly the flow pattern, and the nature of oscillations while varying its intensity. The influence of heat generation/absorption in the presence of uniform [14], or variable [15] magnetic fields has been considered in the case of non-Newtonian fluids. The results obtained indicate that the Lorentz force is a key parameter for controlling the heat transfer within the cavity. The latter is also affected by the heat generation and decreases by raising the power-law index.

According to this preliminary literature review, it appears that there is a lack of studies addressing the numerical modeling in the presence of the Lorentz force and internal heat generation and their impacts on heat transfer generated by thermal convection in confined configurations filled with non-Newtonian fluids. Therefore, the objective of the present investigation is to elucidate the effect of the Hartmann number ($Ha = 0$ to 50), the heat generation ($R = 0$ and 1) and the power-law index ($n = 0.8$ to 1.2) on natural convection within a square cavity partially heated from the bottom wall. The study is conducted using the MRT-LBM for an external Rayleigh number and a Prandtl number fixed at 10^5 and 10, respectively.

2 Mathematical Formulation

2.1 Physical Model

The two-dimensional physical model under consideration is depicted in Fig. 1. It consists of a square cavity partially heated from below. The heating source of length $\varepsilon = w/L = 0.4$ is centrally located ($d/L = 0.5$). The cavity is cooled from its vertical sides, while the remaining walls (the upper horizontal wall and the non-heated elements of its lower wall) are thermally insulated. The cavity is filled with a non-Newtonian fluid ($Pr = 10$) and subject to the action of a horizontal magnetic field of intensity B_0. The fluid flow is laminar, and all thermo-physical properties of the non-Newtonian fluid are assumed to be constant. However, the fluid density is assumed to vary linearly with temperature in the buoyancy term in line with the Boussinesq approximation.

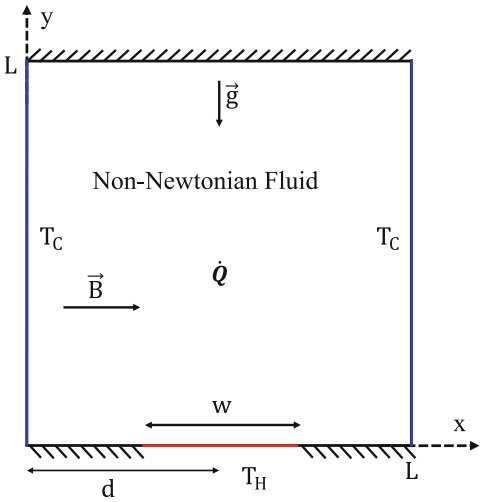

Fig. 1. Schematic of the studied model.

2.2 Lattice Boltzmann Method

The MRT-LBM has been used in previous studies to simulate non-Newtonian fluid flows. This method has many advantages in terms of accuracy, numerical stability, ease of implementation of boundary conditions, and suitability for parallel computing. The LBM equations used to determine the velocity and temperature fields of the non-Newtonian fluid in the presence of two external forces (Lorentz and buoyancy forces) are expressed by Eqs. (1) (for flow) and (2) (for temperature) using the D2Q9 and D2Q5 models, respectively.

$$f(\vec{r} + c_k \Delta t, t + \Delta t) = f(\vec{r}, t) - M^{-1} S\left(m(\vec{r}, t) - m^{eq}(\vec{r}, t)\right) + M^{-1}(\mathbb{I} - S/2)F \quad (1)$$

$$g(\vec{r} + c_k \Delta t, t + \Delta t) = g(\vec{r}, t) - N^{-1} Q\left(n(\vec{r}, t) - n^{eq}(\vec{r}, t)\right) + \omega_k \Phi \quad (2)$$

where $f/(g)$ is the density/(temperature) distributions functions. The function $m_k/(n_k)$ is the moment space of density/(temperature) and $m^{eq}/(n^{eq})$ is its corresponding equilibrium moment space, which is defined as follows:

$$m^{eq} = \begin{pmatrix} \rho, -2\rho + 3\rho\left(u^2 + v^2\right), \rho - 3\rho\left(u^2 + v^2\right), \rho u, \\ -\rho u, \rho v, -\rho v, \rho\left(u^2 - v^2\right), \rho uv \end{pmatrix} \tag{3}$$

$$n^{eq} = (T, uT, vT, -2T, 0) \tag{4}$$

The expressions of the force term F and the source term Φ in Eqs. (1) and (2) are given as following:

$$F = \begin{cases} F_0 = 0 \\ F_1 = 6\rho\left(F_x u + F_y v\right) \\ F_2 = -6\rho\left(F_x u + F_y v\right) \\ F_3 = F_x \\ F_4 = -F_x \\ F_5 = F_y \\ F_6 = -F_y \\ F_7 = 2\rho\left(F_x u - F_y v\right) \\ F_8 = \rho\left(F_y u + F_x v\right) \end{cases} \tag{5}$$

$$\Phi = \frac{\alpha \Delta T}{L^2} R \tag{6}$$

The parameter $R\ (= Ra_I/Ra_E)$ is the source term in the energy equation represented by the ratio between the internal and external Rayleigh numbers and F_x and F_y are the external forces applied in the x-direction and y-direction, respectively. In the present study, these forces are defined as follows:

$$\begin{aligned} Fx &= 0 \\ Fy &= \frac{\alpha^2 Pr Ra_E}{\Delta T L^3}(T - T_0) - \frac{Ha^2 k}{L^{2n}\alpha^{1-n}} v \end{aligned} \tag{7}$$

The physical parameters of the study are:

$$\begin{aligned} &Pr = (\mu_0/\rho)L^{2-2n}/(\alpha^{2-n}),\ Ra_E = g\beta\Delta T L^{2n+1}/\left((\mu_0/\rho)\alpha^n\right), \\ &Ra_I = g\beta\dot{Q}L^{2n+3}/(\lambda(\mu_0/\rho)\alpha^n),\ Ha = B_0 L^n\sqrt{\sigma\alpha^{1-n}/(\mu_0)} \end{aligned} \tag{8}$$

The relaxation diagonal matrices in the Eqs. (1) and (2) are defined as follows:

$$S = diag(1.0, 1.4, 1.4, 1.0, 1.2, 1.0, 1.2, 1/\tau_\vartheta, 1/\tau_\vartheta) \tag{9}$$

$$Q = diag(1.0, 1/\tau_\alpha, 1/\tau_\alpha, 1.0, 1.0) \tag{10}$$

The parameters τ_ϑ and τ_α are the relaxation times, which are related to the dynamic viscosity and thermal diffusivity at the mesoscopic scale through the Chapmann-Enskog expansion analysis as follows:

$$\tau_\vartheta = 3(\mu/\rho) + 0.5 \tag{11}$$

$$\tau_\alpha = 5\alpha + 0.5 \tag{12}$$

In the case of a non-Newtonian fluid, the dynamic viscosity varies locally with the shear rate as follows:

$$\mu = \mu_0 |\dot{\gamma}|^{n-1} \tag{13}$$

With

$$|\dot{\gamma}| = \sqrt{2 S_{\alpha\beta} S_{\alpha\beta}} \tag{14}$$

The parameter $S_{\alpha\beta}$ is the shear stress, defined by Eq. (15) in the MRT model.

$$S_{\alpha\beta} = \frac{-3}{2\rho} \sum C_{\alpha,i} C_{\beta,i} \sum M^{-1} S M \left(f - f^{eq}\right) \tag{15}$$

Classical Bounce-Back boundary conditions have been used to evaluate the unknown density distribution function (inside the physical domain), which is given by Eq. (16), along the motionless cavity walls. The evaluation of the unknown thermal distribution function g along the rigid walls, is expressed by Eq. (17).

$$f_{w,i} = f_{w,\bar{i}} \tag{16}$$

$$g_{w,i} = T_w - \sum_{j=0, j\neq i}^{4} g_{w,j} \tag{17}$$

where i is the direction of distribution function inside physical domain while $\bar{i}$ is its opposite direction along the rigid wall, w.

Finally, the macroscopic density, velocity and temperature are deduced by the expressions given by Eq. (18).

$$\rho = \sum_{k=0}^{8} f_k, \quad \rho\vec{u} = \sum_{k=0}^{8} f_k \vec{c}_k + \Delta t \vec{F}/2, \quad T = \sum_{k=0}^{4} g_k \tag{18}$$

The local/mean Nusselt number along the heating source are evaluated as follows:

$$Nu_L = -\left.\frac{\partial T}{\partial Y}\right|_{Y=0} \text{ and } Nu_m = \frac{1}{\varepsilon} \int_{d-\varepsilon/2}^{d+\varepsilon/2} Nu_L dX \tag{19}$$

2.3 Numerical Validation and Grid Size

The developed MRT-LBM code was submitted to several tests of validation. These tests are restricted here to the case of a cavity filled with a non-Newtonian fluid or submitted to the effect of an external magnetic field. In the case of a non-Newtonian fluid-filled square cavity, we used as reference the results obtained by Turan et al. [16]. The comparative results depicted in Fig. 2 in terms of mean Nusselt number for different rheological behaviors of the working fluid show a good agreement with a maximum difference not exceeding 1.38%. In the presence of an external magnetic field and an internal heat generation, the numerical results are compared to those published by Taghikhani [17] in terms of streamlines (Fig. 3a) and isotherms (Fig. 3b). From these figures, it can be seen that the results obtained with the MRT-LBM code are in very good qualitative and quantitative agreements with those published by Taghikhani [17].

The mesh adopted was preceded by numerous tests to examine its effect on the results. These tests were conducted in terms of Nu_m variations for $Ra_E = 10^5$, $Ha = 50$, $R = 1$ and various n, using the grids 100×100, 160×160, 200×200, 260×260 and 300×300. Based on the results presented in Table 1, the grid 200×200 is considered appropriate in terms of accuracy and computation time. In fact, compared to the finest grid of 300×300, the maximum deviation recorded using the mesh 200×200 is within 0.88% with a substantial gain in terms of calculation time.

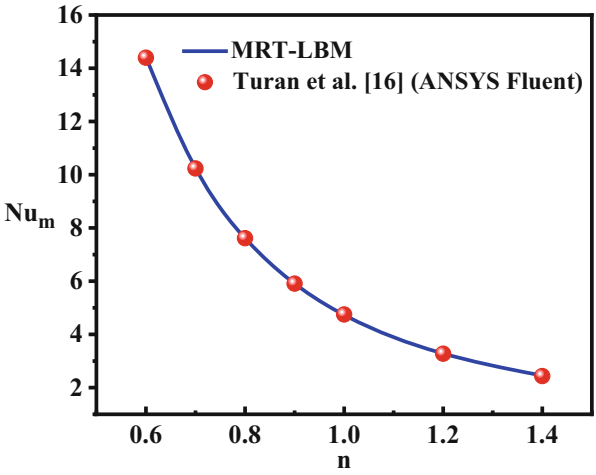

Fig. 2. Validation in terms of mean Nusselt number variations vs. n for $Ra = 10^5$.

3 Results and Discussion

The combined influence of the Hartmann number ($0 \leq Ha \leq 50$), internal heat generation ($R = 0$ and 1) and power law index ($0.8 \leq n \leq 1.2$) on the thermal and dynamic behaviors of the non-Newtonian fluid are described in this section for a fixed external Rayleigh number of 10^5.

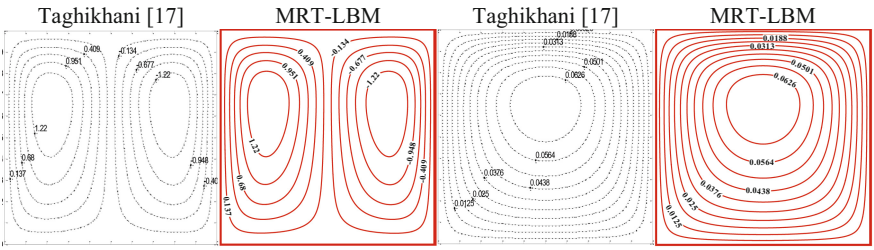

Fig. 3. Validations in terms of streamlines (**a**) and isotherms (**b**) for $Ra_E = 10^6$, $Pr = 0.733$ and $R = 1$.

Table 1. Sensitivity of Nu_m to the grid size for $Ra_E = 10^5$, $Ha = 50$, $R = 1$ and various n.

	100 × 100	160 × 160	200 × 200	260 × 260	300 × 300
$n = 0.8$	5.5673	5.6310	5.6597	5.6925	5.7098
$n = 1.0$	2.0947	2.1155	2.1243	2.1343	2.1393
$n = 1.2$	1.4661	1.4790	1.4843	1.4898	1.4925

3.1 Streamlines and Isotherms

The solutions being symmetrical relative to the vertical cavity's centerline, both streams and isotherms are exemplified in Fig. 4 to illustrate the combined effect of the parameters *Ha* and *n*. By varying either, *Ha* or *n*, the flow symmetry relative to the vertical centerline of the cavity is preserved but the flow intensity undergoes substantial changes. In fact, the fluid flow is organized into two vertical counter-rotating cells of equal intensities filling the inner space of the cavity. For $R = 0$, Fig. 4a shows that both in the presence and in the absence of the Lorentz force, the increase of *n* reduces the flow intensity inside the cavity. Likewise, the intensification of the magnetic field through the increase of *Ha* has a damping effect leading to the attenuation of the flow intensity. Comparatively, the drop in the intensity of the flow that accompanies the augmentation of *n* engenders a slight shift downward of the center of rotation of each cell in the absence of the magnetic field while this shift is more manifest at $Ha = 30$. Quantitatively, the flow intensity for the shear-thinning/(shear-thickening) fluid is 49.40%/48.57% higher/lower than that corresponding to the Newtonian case for $Ha = 0$. These percentages become 76.80%/93.07% at $Ha = 30$. This means that, the higher the fluid's apparent kinematic viscosity, the more it is affected by the Lorentz force. For $R = 1$, value expressing the equality between the internal and external Rayleigh numbers, limited changes (small reductions) are observed while comparing the results to those obtained without internal heat generation ($R = 0$). In fact, the intensification/reduction observed in the flow intensity in comparison with the Newtonian case is reduced to 48.22%/47.95% for a shear-thinning/(shear-thickening) fluid at $Ha = 0$ and 68.05%/92.95% at $Ha = 30$. From another perspective, increasing *R* has a limited impact on the flow intensity for $n =$

1.2. Quantitatively, for $Ha = 0$, the flow intensity decreases by about 3.37%/1.11% for $n = 0.8/1.0$ by increasing R from 0 to 1. However, the effect of heat generation becomes increasingly important for the shear-thinning fluid in the presence of the magnetic field since the same increase of R leads to a decay of the flow intensity by about 27% for $n = 0.8$ at $Ha = 30$.

The thermal aspect of the problem, illustrated in Fig. 4 in terms of isotherms, shows that in the absence of magnetic field, the increase of n induces a relaxation of the isotherms next to the top sides of the heat evacuating walls and accentuates the length of thermal plume above the heated element. Also, as a result of convection attenuation accompanying the increase of n and Ha, the thermal plume and the vertical thermal boundary layers observed next to the cold walls increase in thickness with such parameters. The important transformations engendered by increasing n and Ha are observed in the case of shear-thickening fluid which almost recovers the diffusive regime at $Ha = 30$. Globally, the lower the consistency index, the less the temperature distribution is impacted by the intensification of Ha. At $R = 1$, a trend towards temperature uniformity within the cavity is observed for the different rheological behaviors of the fluid and the distortion of the isotherms is increasingly attenuated by increasing Hartmann number.

3.2 Heat Transfer

The effect of Hartmann number on the mean Nusselt number is illustrated in Fig. 5 in the absence and in the presence of internal heat generation and various values of n characterizing the change in the non-Newtonian behavior of the fluid. The analysis of the results presented in this figure shows different behaviors (depending on the nature of the fluid) resulting from the variation of Ha. In fact, for the shear-thinning index, the effect of Ha stays limited and leads to a slight decrease of Nu_m for both values of R. Comparatively, the Newtonian fluid is shown to be more sensitive to the variation of Ha. The increase of the latter parameter engenders a degradation of Nu_m with a quasi-linear trend and an important decay slope. Despite the weakening of the intensity of the flow caused by the rise of Ha, the maximum value considered in this study for this parameter ($Ha = 50$) does not bring the fluid back to rest. Finally, the most important effect of Ha is observed in the case of shear-thickening index; the mean Nusselt number decay is drastic by increasing Ha from 0 to 10 (the presence of heat generation accentuates Nu_m attenuation for the latter increase of Ha) and the diffusive regime prevails from $Ha = 20$ for both values of R.

4 Conclusion

Natural convection heat transfer in a square enclosure locally heated by a heating sink symmetrically located on the bottom wall and cooled from the vertical sides has been investigated numerically using the MRT-LBM. The working fluid has a non-Newtonian behavior obeying a power law (or Ostwald) model. The study has focused mainly on the effect of the magnetic field (Ha), the rheological behavior of fluid (n), and in a lesser extent on the internal heat generation whose intensity was varied in a short range. The results presented show that the effect of natural convection is intensified by decreasing

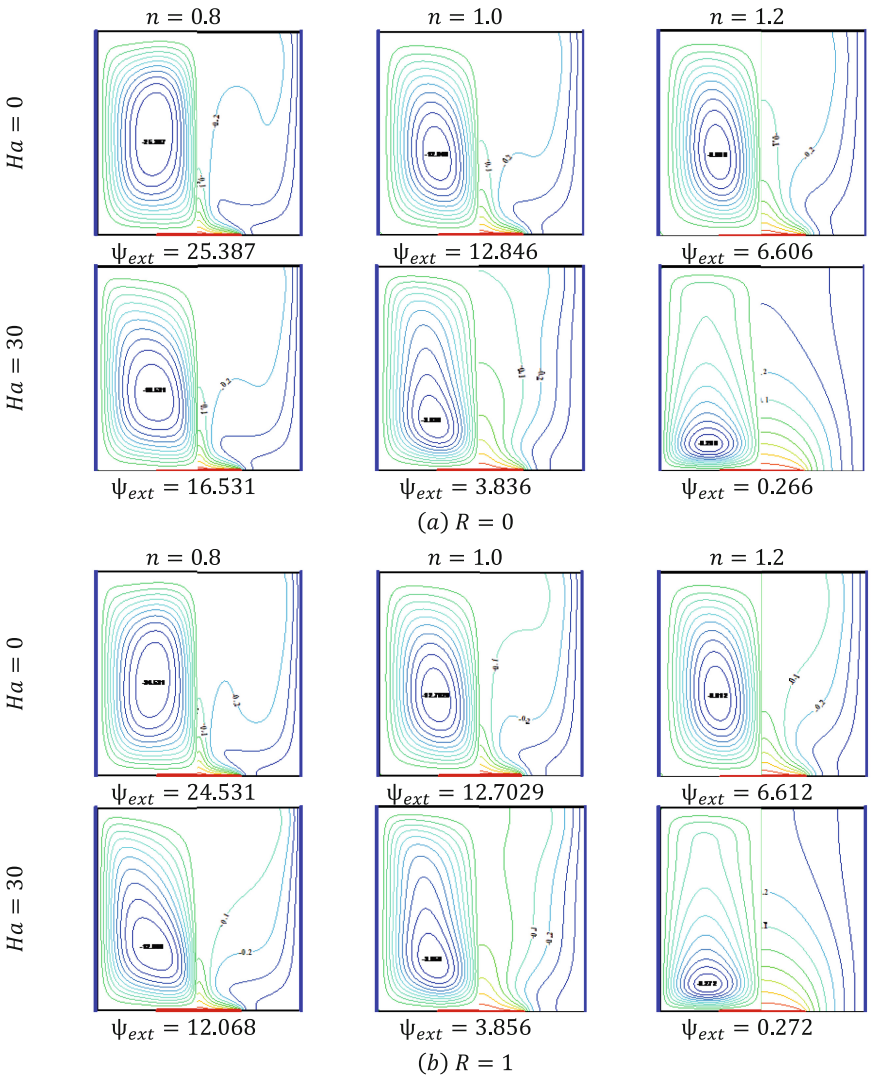

Fig. 4. Streamlines/Isotherms for (*a*) $R = 0$ and (*b*) $R = 1$ and various *Ha* and *n*.

n. The greatest attenuation rate accompanying the increase of Hartmann number, in terms of flow intensity and mean Nusselt number, is observed in the case of shear-thickening fluid. Globally, the internal heat generation has preserved the trends of Nu_m in their variations vs. *Ha* with a perceptible decay compared to $R = 0$. For $n = 1.2$, the presence of heat generation accentuates heat transfer drop when *Ha* goes from 0 to 10. Finally, the symmetry exhibited by the flow structure and the isotherms relative to the vertical cavity's centerline has been preserved while varying the controlling parameters in their respective ranges.

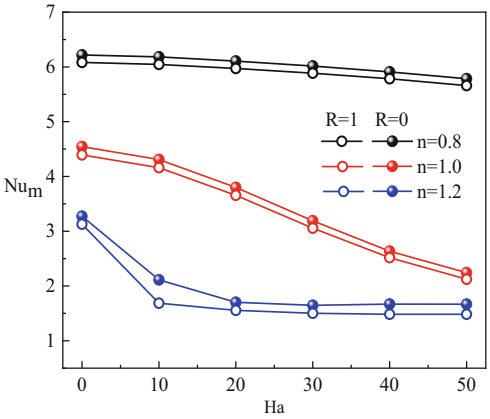

Fig. 5. Variations of the mean Nusselt number vs. *Ha* for various n and $R = 0$ and 1.

Acknowledgment. The authors would like to thank the Partnership Hubert Curien (PHC) Maghreb N°45990SH for its financial support.

Nomenclature

B_0	Magnetic field strength, [T]
c_k	Discrete velocity
f_k/g_k	Density/temperature distribution function
f_k^{eq}/g_k^{eq}	Equilibrium density/temperature distribution function
g	Gravitational acceleration, $\left[\mathrm{m\ s^{-2}}\right]$.
Ha	Hartmann number
$\mathrm{Ra}_E/\mathrm{Ra}_\mathrm{I}$	External/internal Rayleigh number
T	Dimensionless temperature, $(\mathrm{T} - \mathrm{T}_0)/(\mathrm{T}_\mathrm{H} - \mathrm{T}_\mathrm{C})$

Greek Symbols

α	Thermal diffusivity, $\left[\mathrm{m^2 s^{-1}}\right]$
ε	Length of heating source
μ_0	Consistency, $\left[\mathrm{m\ Pa\ s^n}\right]$
ν	Apparent kinematic viscosity, $\left[\mathrm{m^2\ s^{-1}}\right]$
ρ	Density, $\left[\mathrm{Kg\ m^{-3}}\right]$
Ψ	Stream function
w	Weighting factor

Index

H	Hot
C	Cold

References

1. Makayssi, T., Lamsaadi, M., Kaddiri, M.: Natural double-diffusive convection for the Carreau shear-thinning fluid in a square cavity submitted to horizontal temperature and concentration gradients. J. Nonnewton. Fluid Mech. **297**, 104649 (2021)
2. Zheng, Y., Zhang, X., Nouri, M., et al.: Atomic rheology analysis of the external magnetic field effects on nanofluid in non-ideal microchannel via molecular dynamic method. J. Therm. Anal. Calorim. **143**, 1655–1663 (2021)
3. Kefayati, G.H.R.: FDLBM simulation of magnetic field effect on natural convection of non-Newtonian power-law fluids in a linearly heated cavity. Powder Technol. **256**, 87–99 (2014)
4. Kefayati, G.R.: Mesoscopic simulation of magnetic field effect on natural convection of power-law fluids in a partially heated cavity. Chem. Eng. Res. Des. **94**, 337–354 (2015)
5. Kefayati, G.R.: Simulation of heat transfer and entropy generation of MHD natural convection of non-Newtonian nanofluid in an enclosure. Int. J. Heat Mass Transf. **92**, 1066–1089 (2016)
6. Aghakhani, S., Pordanjani, A.H., Karimipour, A., Abdollahi, A., Afrand, M.: Numerical investigation of heat transfer in a power-law non-Newtonian fluid in a C-Shaped cavity with magnetic field effect using finite difference lattice Boltzmann method. Comput. Fluids **176**, 51–67 (2018)
7. Zhang, R., Aghakhani, S., Pordanjani, A.H., Vahedi, S.M., Shahsavar, A., Afrand, M.: Investigation of the entropy generation during natural convection of Newtonian and non-Newtonian fluids inside the L-shaped cavity subjected to magnetic field: application of lattice Boltzmann method. Eur. Phys. J. Plus. **135** (2020)
8. Acharya, S., Goldstein, R.J.: Natural convection in an externally heated vertical or inclined square box containing internal energy sources. J. Heat Transf. **107**, 855–866 (1985)
9. Fusegi, T., Hyun, J.M., Kuwahara, K.: Natural convection in a differentially heated square cavity with internal heat generation. Numer. Heat Transf. Part A Appl. **21**, 215–229 (1992)
10. Kandaswamy, P., Nithyadevi, N., Ng, C.O.: Natural convection in enclosures with partially thermally active side walls containing internal heat sources. Phys. Fluids **20**, 1–10 (2008)
11. Khanafer, K.M., Chamkha, A.J.: Hydromagnetic natural convection from an inclined porous square enclosure with heat generation. Numer. Heat Transf. Part A Appl. **33**, 891–910 (1998)
12. Hasnaoui, S., Amahmid, A., Raji, A., Beji, H., Hasnaoui, M., Dahani, Y., Benhamed, H.: Double-diffusive natural convection in an inclined enclosure with heat generation and Soret effect, Eng. Comput. (Swansea, Wales). **35**, 2753–2774 (2018)
13. Hasnaoui, S., Amahmid, A., Raji, A., Beji, H., El Mansouri, A., Hasnaoui, M.: LBM simulation of stabilizing/destabilizing effects of thermodiffusion and heat generation in a rectangular cavity filled with a binary mixture. Int. Commun. Heat Mass Transf. **126**, 105417 (2021)
14. Nemati, M., Sani, H.M., Chamkha, A.J.: Optimal wall natural convection for a non-Newtonian fluid with heat generation/absorption and magnetic field in a quarter-oval inclined cavity. Phys. Scr. **96** (2021)
15. Nemati, M., Sefid, M., Sajadi, A.M., Ghaemi, F., Baleanu, D.: Lattice Boltzmann method to study free convection and entropy generation of power-law fluids under influence of magnetic field and heat absorption/generation, J. Therm. Anal. Calorim. (2022)
16. Turan, O., Sachdeva, A., Chakraborty, N., Poole, R.J.: Laminar natural convection of power-law fluids in a square enclosure with differentially heated side walls subjected to constant temperatures. J. Nonnewton. Fluid Mech. **166**, 1049–1063 (2011)
17. Taghikhani, M.A.: Magnetic field effect on natural convection flow with internal heat generation using fast Ψ-Ω method. J. Appl. Fluid Mech. **8**, 189–196 (2015)